Underwater shock wave induced by pulsed discharge on water

Tomohiro Furusato[1], Mitsuru Sasaki[2], Yoshinobu Matsuda[1], and Takahiko Yamashita[1]

[1] Graduate School of Engineering, Nagasaki University, Nagasaki 852-8521, Japan
[2] Institute of Industrial Nanomaterials, Kumamoto University, Kumamoto 860-8555, Japan

E-mail: t-furusato@nagasaki-u.ac.jp

Received xxxxxx
Accepted for publication xxxxxx
Published xxxxxx

Abstract

Plasmas on liquids have provided significant applications in material, environmental, and biological sciences. The mechanisms of these chemical reactions in liquids have been primarily discussed by the plasma–liquid interactions and convection by an electrohydrodynamic flow. Although shock waves play a significant role in the radical formation, agitation, and cell destruction, not much information is available on underwater shock waves induced by the surface discharge on water. In this study, an underwater shock wave generated by the pulsed surface discharge on water using the laser shadowgraph method has been demonstrated. The results reveal that the shock wave generated by the discharge on water was transmitted into the water. The mean velocity of the shock wave reached 1.7 km/s. The results indicate that the surface discharge accelerates the reaction in the water by the combined action of the underwater shock wave and the plasma reaction at the air–water interface. The results are expected to aid in the understanding the mechanisms of existing applications, such as decomposition, synthesis, and sterilization.

Keywords: plasma–liquid interactions, underwater shock waves, surface discharge on water

1. Introduction

Elucidation of the plasma–liquid interaction is of importance for widespread applications in the material, environmental, and biological sciences [1]. The hydrodynamic effect of plasma on liquid is a significant subject because the convection in the liquid facilitates the diffusion of reactive species generated by the plasma. A well-known bulk liquid motion called the electrohydrodynamic (EHD) flow is induced in the form of a plasma jet or streamer discharge (ionic wind) [2–5]. The essential contribution to the bulk liquid motion is the shear stress by the gas flow at the gas–liquid interface [6–8]. In contrast, underwater shock waves act as chemical reactions in water because the shock wave causes plasma formation due to cavitation bubbles, agitation, and mechanical stress to the dissolved material [9,10]. Generally, underwater shock waves have been frequently observed by direct discharge in water [11–13]. However, there are a few studies on underwater shock waves caused by the discharge on water. The detailed observation of the shock waves by surface discharge on water is significant from the viewpoint of understanding the essential reaction mechanisms in existing applications. There is a possibility that the shock waves have acted in addition to the plasma–liquid interactions in previous studies of sterilization [14,15], decomposition [16–19], synthesis [20], and plant cultivation [21] by surface discharge on water.

This study aimed to observe the underwater shock wave

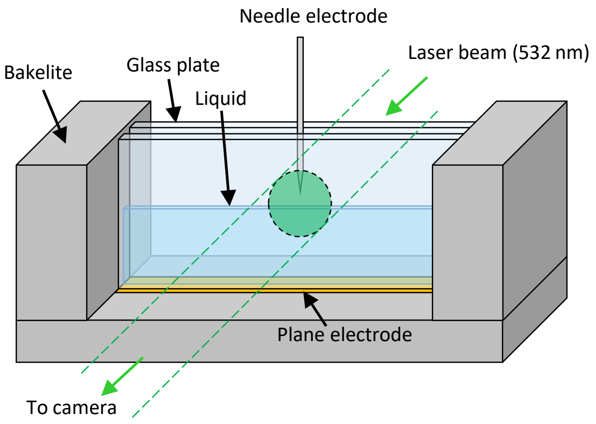

(a)

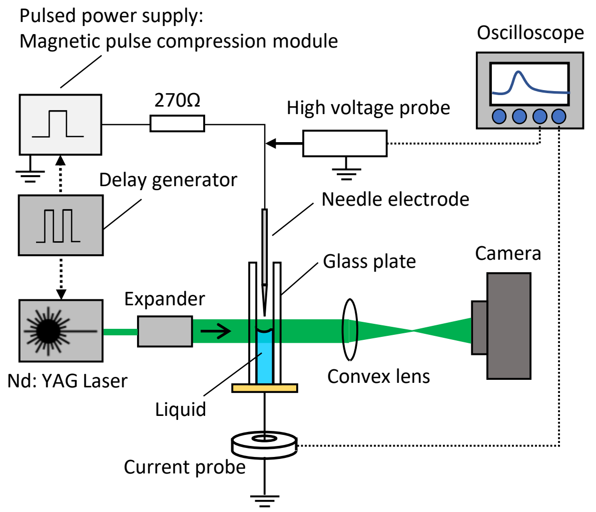

(b)

Figure 1. Experimental setup for the observation of the trajectory-controlled surface discharge on water by the shadowgraph method. (a) High voltage pulsed power supply and the shadowgraph observation system. (b) Side view of the discharge reactor.

induced by pulsed surface discharge on water using a laser shadowgraph method. A positive pulsed voltage was applied to a needle, which was arranged immediately above water, to generate a pulsed surface discharge on the water. The glass container, which limited the discharge path, was developed to observe the two-dimensional shadowgraph images because the surface discharge on water grows radially under the uncontrolled trajectory of the discharge [22,23].

2. Experimental setup

Figure 1 (a) shows an illustration of the discharge reactor. The trajectory of the surface discharge on water was limited to the direction of one dimension by generating the plasma on the narrow water channel of 2 mm between parallel quartz glasses. The needle with a diameter of 1 mm was installed in the space between the quartz glasses to avoid contacting its wall surface. The plane electrode at the bottom of the water was ground. The conductivity of the water was adjusted by dissolving potassium chloride (KCl) and was set to 1 mS/cm. The water depth was approximately 10 mm. The circular pulsed laser beam (Nd: YAG laser; Continuum Co. Ltd.; wavelength: 532 nm; pulse width: 5±2 ns; diameter of circular beam: 25 mm) was directed to pass through the region of the reactor, including the needle tip, air–water surface, and water. The laser shadowgraph image was captured using a digital CMOS camera (D610, Nikon Co. Ltd.). Figure 1 (b) shows the experimental setup. A positive pulsed voltage was applied to the needle electrode made from tungsten using a magnetic pulse compression circuit (MPC3010S-25LP, Suematsu Denshi Co. Ltd.). The detailed topology of the circuit was expressed in a previous study [24]. The applied voltage at the needle electrode was measured with a high-voltage probe (HV-P30, Iwatsu Co., Ltd.). The current at the ground side of the reactor was measured using a current monitor (Model 4100, Pearson Electronics Co. Ltd.). The waveforms were observed using an oscilloscope (DPO-4104-L, Textronix Co., Ltd.). The delay generator synchronized the Nd: YAG laser and the magnetic pulse compression circuit.

3. Experimental results and discussion

3.1 Voltage and current waveforms

Figure 2 shows the applied voltage and current waveforms. The peak of the applied voltage and current were approximately 27 kV and 22 A, respectively. The initiation of the shock wave from the discharge channel was investigated by varying the shooting time of the shadowgraph image considering that $t = 0$ when the current starts to flow.

3.2 Time-resolved shadowgraph images of underwater shock waves by surface discharge on water

Figures 3 (a)–(c) show the shadowgraph images with a time resolution of 5±2 ns. The discharge branched two ways from the needle electrode and propagated on the water surface in

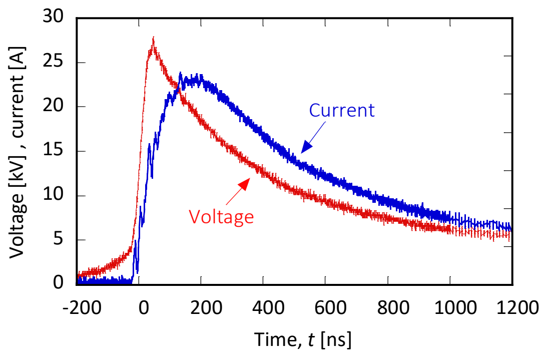

Figure 2. Voltage and current waveforms while the pulsed surface discharge is occurring on the water.

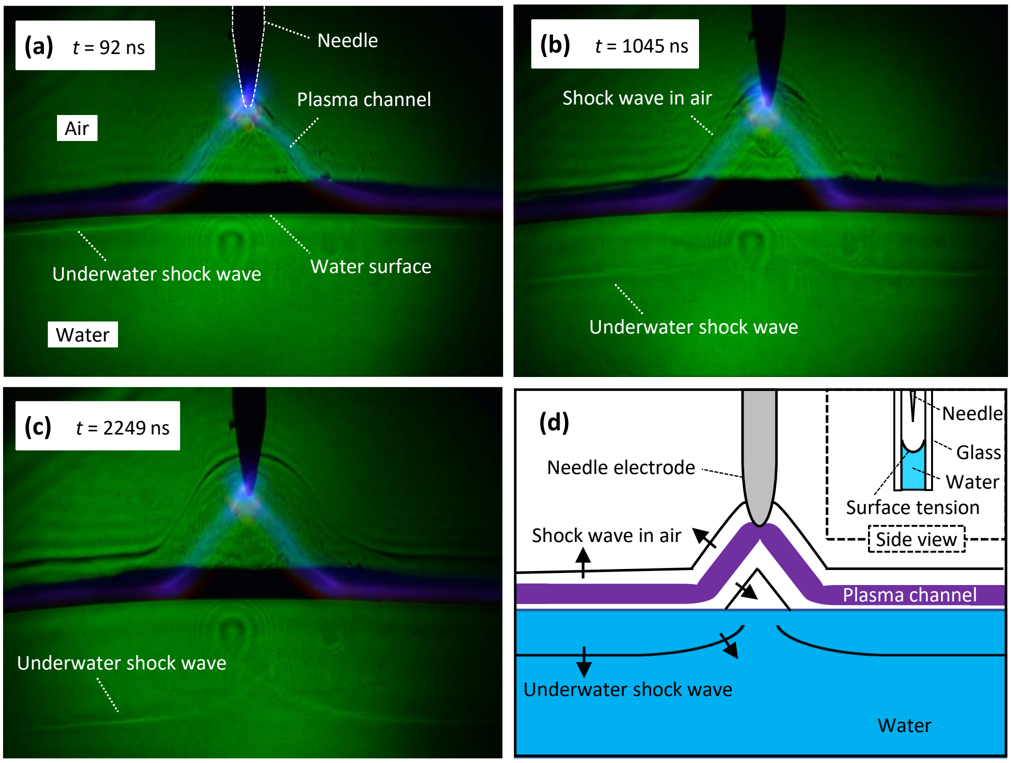

Figure 3. Time-resolved shadowgraph images under post-ignition of the surface discharge on water. The time t in (a)–(c) is the time from the initiation of the current flow; (d) shows an illustration of the shock wave propagation in air and water from the plasma channel.

the opposite direction each other. The instability of the gas-liquid interface due to the surface discharge was not observed in Figs. 3(a)–(c) because of the high-speed phenomenon within a few microseconds. Figure 3 (d) shows an illustration of the shadowgraph image (Fig. 3 (b)). Shock waves were clearly observed in the air and water. The dark region at the boundary between the air and water in Figs. 3 (a)–(c) is due to the surface tension of water, as shown in the upper right of Fig. 3(d). The laser across the boundary at the air–water interface

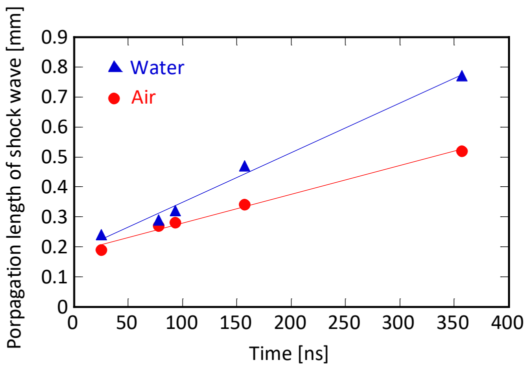

Figure 4. Time evaluation of the propagation length of the shock wave in air and water. The propagation lengths of the shock wave mean the distance from the plasma to the shock front in air and from the water surface to the shock front in water, respectively.

is scattered because of the gradient of the water surface due to the surface tension. Figure 4 shows the propagation length of the shock waves in air and water as a function of time. The Mach numbers were 2.6 in air and 1.1 in water. Here, the focus was on the fact that the shock wave in air started to propagate within 100 ns, as shown in Fig. 3 (a). The generation of the shock waves is closely related to the heating mechanism of the discharge. The shock wave generation within 100 ns is consistent with an ultra-fast gas heating, the reactions of which are dissociative quenching of the electronically excited nitrogen molecules N_2 ($B^3\ \Pi_g$, $C^3\Pi_u$) and O (^1D) in the order of a dozen nanoseconds [25]. Additionally, a shock wave initiation in the atmospheric pressure air was observed immediately after the arc discharge ignition at the pin-to-pin electrode (~130 ns) [26]. The rapid vibration-to-translation (V-T) relaxation of the equilibrated stretching H_2O (ν_1, ν_3) (~ 100 ns) and the exothermicity of the OH formation reaction contribute to the fast gas heating [27].

3.3 Shock wave propagation from air into water

The ultra-fast gas heating mechanism indicates that the shock waves in the air are generated extremely early within 100 ns, which affect the generation of the underwater shock wave. The initiation time of the underwater shock wave corresponds to the shock wave generation time (~ 100 ns) in air, as shown in Fig. 4. In general, an acoustic impedance mismatch should be considered for having a huge mismatch, such as an air–water interface. The coefficient of power reflection, R_w, is as follows:

$$R_w = R_p^2, \quad (1)$$

$$R_p = \frac{Z_2 - Z_1}{Z_2 + Z_1}, \quad (2)$$

where, R_p is the coefficient of reflection, the acoustic impedance at 25 °C for air is Z_1 = 409 kg s m^{-2} and for water is Z_2 = 1.49×10^6 kg s m^{-2}. Consequently, the incident longitudinal wave from air to water is almost reflected because R_w is 0.999. However, the impedance matching theory is generally available for ultrasound and has not been sufficiently verified for shock waves. Here, the transmission of shock waves into water is discussed. The impedance mismatch can be relaxed by increasing the water temperature owing to the ion incident because the acoustic impedance decreases with increasing the water temperature. The effect of incident ions, which was accelerated by cathode fall region, formed on the water surface on the water temperature was analyzed using the classical molecular dynamics simulation [28]. The simulated results indicated that the incident of ions creates a temperature gradient at the water surface, and the water temperature reaches 1100 K on the surface layer (10 Å) at an incident ion energy of 100 eV. The transmission of the shock wave into the water can be explained by t

he gradient of the water temperature, which corresponds to the acoustic impedance. Conversely, an observation was made of the underwater shock wave induced by the transmission of a blast wave (Mach number: 4.1) from air to water [29]. In our study, the shock wave generated in the plasma channel propagates via the cathode fall region between the plasma and water surface. The shock wave immediately reaches the water because the distance of the cathode fall region on the water is a few tens to a hundred μm [30,31]. In other words, an intense shock wave acts on the water surface because of the extremely small cathode fall distance. As stated above, the transmission of the shock waves into the water is achieved by increasing the water temperature owing to the incident of ions and the propagating shock wave at a small distance from the cathode fall.

4. Conclusions

In conclusion, it was found that the pulsed surface discharge on water can cause underwater shock waves. The experimental results indicate that the shock wave generated by the surface discharge is transmitted into the water, irrespective of the large difference in acoustic impedance between the air and water. The discovery of the underwater shock wave generated by the surface discharge will be helpful to elucidate the plasma-liquid interaction, which will contribute to constructing accurate simulations in the future. The surface discharge on water has advantages for industrial applications. A direct discharge in water may cause water pollution due to erosion of the electrodes; however, the surface discharge on the water does not cause water pollution because the electrodes are placed outside the aqueous solution. Furthermore, since the discharge duration of this experimental system is in microseconds, the electrolytic behavior of the ground electrode immersed in water can be suppressed compared to DC discharge. These findings help to improve the existing applications, for example, sterilization, polymetric synthesis, and organic decomposition, because plasma chemical reactions in liquid, combining shock wave effects, increase with high repetition of pulsed discharges and increasing discharge current.

References

[1] Bruggeman P J, Kushner M J, Locke B R, Gardeniers J G E, Graham W G, Graves D B, Hofman-Caris R C H M, Maric D, Reid J P, Ceriani E, Fernandez Rivas D, Foster J E, Garrick S C, Gorbanev Y, Hamaguchi S, Iza F, Jablonowski H, Klimova E, Kolb J, Krcma F, Lukes P, MacHala Z, Marinov I, Mariotti D, Mededovic Thagard S, Minakata D, Neyts E C, Pawlat J, Petrovic Z L, Pflieger R, Reuter S, Schram D C, Schröter S, Shiraiwa M, Tarabová B, Tsai P A, Verlet J R R, Von Woedtke T, Wilson K R, Yasui K and Zvereva G 2016 Plasma-liquid interactions: A review and roadmap *Plasma Sources Sci. Technol.* **25** 053002

[2] Van Rens J F M, Schoof J T, Ummelen F C, Van Vugt D C, Bruggeman P J and Van Veldhuizen E M 2014 Induced liquid phase flow by RF Ar cold atmospheric pressure plasma jet *IEEE Trans. Plasma Sci.* **42** 2622–3

[3] Kanazawa S, Kawano H, Watanabe S, Furuki T, Akamine S, Ichiki R, Ohkubo T, Kocik M and Mizeraczyk J 2011 Observation of OH radicals produced by pulsed discharges on the surface of a liquid *Plasma Sources Sci. Technol.* **20** 034010

[4] Shimizu T, Iwafuchi Y, Morfill G E and Sato T 2011 Formation of thermal flow fields and chemical transport in air and water by atmospheric plasma *New J. Phys.* **13** 053025

[5] Lai J, Petrov V and Foster J E 2018 Understanding Plasma-Liquid Interface Instabilities Using Particle Image Velocimetry and Shadowgraphy Imaging Methods *IEEE Trans. Plasma Sci.* **46** 875–81

[6] Verlackt C C W, Van Boxem W and Bogaerts A 2018 Transport and accumulation of plasma generated species in aqueous solution *Phys. Chem. Chem. Phys.* **20** 6845–59

[7] Lindsay A, Anderson C, Slikboer E, Shannon S and Graves D 2015 Momentum, heat, and neutral mass transport in convective atmospheric pressure plasma-liquid systems and implications for aqueous targets *J. Phys. D: Appl. Phys.* **48** 424007

[8] Ohyama R, Inoue K and Chang J S 2007 Schlieren optical visualization for transient EHD induced flow in a stratified dielectric liquid under gas-phase ac corona discharges *J. Phys. D: Appl. Phys.* **40** 573–8

[9] Gupta S B and Bluhm H 2007 Pulsed underwater corona discharges as a source of strong oxidants: OH and H_2O_2 *Water Sci. Technol.* **55** 7–12

[10] Lukes P, Sunka P, Hoffer P, Stelmashuk V, Pouckova P, Zadinova M, Zeman J, Dibdiak L, Kolarova H, Tomankova K, Binder S and Benes J 2014 Focused tandem shock waves in water and their potential application in cancer treatment *Shock Waves* **24** 51–7

[11] An W, Baumung K and Bluhm H 2007 Underwater streamer propagation analyzed from detailed measurements of pressure release *J. Appl. Phys.* **101** 053302
[12] Oshita D, Hosseini S H R, Okuda Y, Miyamoto Y, Sakugawa T, Katsuki S and Akiyama H 2012 Time-resolved high-speed visualization and analysis of underwater shock wave focusing generated by a magnetic pulse compression unit *IEEE Trans. Plasma Sci.* **40** 2395–400
[13] Marinov I, Starikovskaia S and Rousseau A 2014 Dynamics of plasma evolution in a nanosecond underwater discharge *J. Phys. D: Appl. Phys.* **47** 224017
[14] Lukes P, Dolezalova E, Sisrova I and Clupek M 2014 Aqueous-phase chemistry and bactericidal effects from an air discharge plasma in contact with water: Evidence for the formation of peroxynitrite through a pseudo-second-order post-discharge reaction of $H_2O_2$and HNO_2 *Plasma Sources Sci. Technol.* **23** 015019
[15] Yang D Z, Jia L, Wang W C, Wang S, Jiang P C, Zhang S, Yu Q X and Chen G L 2014 Atmospheric pressure gas-liquid diffuse nanosecond pulse discharge used for sterilization in sewage *Plasma Process. Polym.* **11** 842–9
[16] Sato M, Tokutake T, Ohshima T and Sugiarto A T 2008 Aqueous phenol decomposition by pulsed discharges on the water surface *IEEE Trans. Ind. Appl.* **44** 1397–402
[17] Hayashi Y, Wahyudiono, Machmudah S, Takada N, Kanda H, Sasaki K and Goto M 2014 Decomposition of methyl orange using pulsed discharge plasma at atmospheric pressure: Effect of different electrodes *Jpn. J. Appl. Phys.* **53** 010212
[18] Takeuchi N, Mizuki A and Yasuoka K 2015 Investigation of the loss mechanisms of hydroxyl radicals in the decomposition of organic compounds using plasma generated over water Generation of ozone by corona discharge and implications for aqueous targets of organic compounds using plasma generated *Jpn. J. Appl. Phys.* **54** 116201
[19] Mededovic Thagard S, Stratton G R, Dai F, Bellona C L, Holsen T M, Bohl D G, Paek E and Dickenson E R V 2017 Plasma-based water treatment: Development of a general mechanistic model to estimate the treatability of different types of contaminants *J. Phys. D: Appl. Phys.* **50** 014003
[20] Hirano Y, Miyanomae R, Sasaki M, Quitain A T, Kida T and Okubayashi S 2016 New Route for the Production of Thermosensitive Polymer with Pulsed Arc Discharge at the Argon-Water Interface *IEEE Trans. Plasma Sci.* **44** 211–5
[21] Takahata J, Takaki K, Satta N, Takahashi K, Fujio T and Sasaki Y 2015 Improvement of growth rate of plants by bubble discharge in water *Jpn. J. Appl. Phys.* **54** 01AG07
[22] Furusato T, Obata D, Yota Y and Takahiko Y 2018 A New Evaluation Method of Contact Area at Interface between Pulsed Surface Discharge and Water *IEEE Trans. Plasma Sci.* **46** 2079–84
[23] Furusato T, Sadamatsu T, Matsuda Y and Yamashita T 2017 Streamer Branching and Spectroscopic Characteristics of Surface Discharge on Water Under Different Pulsed Voltages *IEEE Trans. Plasma Sci.* **45** 711–7
[24] Furusato T, Ashizuka N, Kamagahara T, Matsuda Y, Yamashita T, Sasaki M, Kiyan T and Inada Y 2018 Anomalous plasma temperature at supercritical phase of pressurized CO_2 after pulsed breakdown followed by large short-circuit current *IEEE Trans. Dielectr. Electr. Insul.* **25** 1807–13
[25] Popov N A 2016 Pulsed nanosecond discharge in air at high specific deposited energy: Fast gas heating and active particle production *Plasma Sources Sci. Technol.* **25** 44003
[26] Lo A, Cessou A, Lacour C, Lecordier B, Boubert P, Xu D A, Laux C O and Vervisch P 2017 Streamer-to-spark transition initiated by a nanosecond overvoltage pulsed discharge in air *Plasma Sources Sci. Technol.* **26** 045012
[27] Komuro A and Ono R 2014 Two-dimensional simulation of fast gas heating in an atmospheric pressure streamer discharge and humidity effects *J. Phys. D: Appl. Phys.* **47** 155202
[28] Minagawa Y, Shirai N, Uchida S and Tochikubo F 2014 Analysis of effect of ion irradiation to liquid surface on water molecule kinetics by classical molecular dynamics simulation *Jpn. J. Appl. Phys.* **53** 010210
[29] Hosseini H, Moosavi-Nejad S, Akiyama H and Menezes V 2014 Shock wave interaction with interfaces between materials having different acoustic impedances *Appl. Phys. Lett.* **104** 103701
[30] Mezsei P, Cserfalvi T and Janossy M 1998 The gas temperature in the cathode surface - dark space boundary layer of an electrolyte cathode atmospheric glow discharge (ELCAD) The gas temperature in the cathode surface — dark space boundary layer of an electrolyte cathode at *J. Phys. D: Appl. Phys.* **31** L41–2
[31] Mezsei P and Cserfalvi T 2006 The investigation of an abnormal electrolyte cathode atmospheric glow discharge (ELCAD) *J. Phys. D: Appl. Phys.* **39** 2354–539